SPACE-TIME SIGNAL SUBSPACE ESTIMATION FOR WIDE-BAND ACOUSTIC ARRAYS

Elio D. Di Claudio(*) *and Giovanni Jacovitti*(**)

DIET, Department of Information Engineering, Electronics and Telecommunications
University of Rome "La Sapienza", Via Eudossiana, 18, I-00187 Rome, Italy
Phone: (*) +39-06-44585490, (**) +39-06-44585838; Fax: +39-06-4873300
Email: (*) elio.diclaudio@diet.uniroma1.it, (**) giovanni.iacovitti@diet.uniroma1.it.

ABSTRACT

Acoustic array applications are generally characterized by very large signal bandwidth. Most existing wide-band direction of arrival (DOA) estimators are based on binning in the frequency domain, so that within each bin the signal model is considered approximately narrow-band. In this work the basic inconsistency of the commonly used binning is first shown. It is shown that the recent Space Time MUSIC (ST-MUSIC) method, which estimates a set of narrow-band signal subspaces directly from the space-time array covariance and combines them within a Weighted Subspace Fitting paradigm, can restore wide-band DOA estimation consistency in most scenarios, obtaining a large variance improvement at high signal to noise ratio (SNR). In addition, a refined ST-MUSIC subspace weighting is proposed to improve accuracy, especially at low SNR.

***Index Terms*—** Acoustic array, Wide-band direction finding, Weighted Subspace Fitting, ST-MUSIC, UWB communications.

1. INTRODUCTION

Direction of Arrival (DOA) estimation of multiple, wide-band sources by a sensor array is a relevant topic of research in acoustic signal processing [1], essential for many applications including sound recording, hands free communications, acoustic surveillance, noise cancellation, noise mapping, acoustic ecology, etc… Most efficient multi-source wide-band DOA estimators perform channelization (*frequency binning*) of array outputs by the Discrete Fourier Transform (DFT) or a filter bank, so that each bin *approximately* satisfies the narrow-band model [2], [3], [4]. A *Spatial Correlation Matrix* (SCM) is estimated for each bin and used in a multi-band approximate Maximum Likelihood (ML) [2] or Weighted Subspace Fitting (WSF) estimator [4], [5] or a coherent focusing (CF) stage [6], [7], [8] to gather all the statistical information about DOA parameters.

The typical short-term stationarity of acoustic wide-band signals may require to employ too few samples for each bin and/or excessive fractional bin bandwidth. The *non-constant steering vector* within each bin and the *spectral leakage* among adjacent bins distort the ideal, finite rank SCM eigen-spectrum [5] creating *spatially spread, ghost* un-calibrated sources [7], [8] and bias. Moreover, the same signal components leaking in different bins are focused in different ways by *focusing matrices*, producing additional source spreading or even splitting. Such mis-modeling generates a DOA estimation variance *plateau* for high signal to noise ratio (SNR), which means that binning based estimators *are not consistent* and *do not approach the theoretical accuracy* of coherent wide-band DOA estimates [7], [8].

The paper is organized as follows. After a notation Sect. 2, in Sect. 3 the basic inconsistency of classical binning is shown with reference to a more realistic convolutional array model. In Sect. 4 the recent [10] *Space-Time MUSIC* (ST-MUSIC) wide-band *signal subspace* estimator is shown capable to restore the consistency by *perfectly* nulling spectral leakage in most cases, starting from the eigen-decomposition of the *Space Time Covariance Matrix* (STCM) of wide-band array outputs, advocated in [11] for its better statistical stability and lower bias with short data records. ST-MUSIC subspaces are weighted according to statistical analysis and can be used in any wide-band WSF [2] or CF [7] DOA estimator. In Sect. 5 a subspace weighting (ST-MUSIC II) scheme minimizing noise effects [5] is introduced. Computer simulations in Sect. 6 demonstrate the largely improved performance of ST MUSIC estimators at high SNR with respect to the classical CF approach using SCM [6], [7]. In addition, ST-MUSIC II restores the accuracy at low SNR with respect to the earlier ST-MUSIC [10], up to the levels of classical CF. Conclusion is drawn in Sect. 7.

2. NOTATION

Throughout the paper, matrices are indicated by capital boldface letters, vectors by lowercase, boldface letters.

The transpose of matrix $\mathbf{A}$ is $\mathbf{A}^T$. The Hermitian transpose of $\mathbf{A}$ is $\mathbf{A}^H$. $\text{trace}(\mathbf{A})$ is the trace of $\mathbf{A}$. $\mathbf{I}_m$ is the square identity matrix of size m. $E[.]$ indicates the expected value. $j=\sqrt{-1}$ is the imaginary unit. The operator $\mathbf{A}=\text{diag}(\mathbf{a})$ creates a diagonal matrix $\mathbf{A}$ from vector $\mathbf{a}$ with $\mathbf{A}(k,k)=\mathbf{a}(k)$. δ_{kl} is the Kronecker delta. Sample estimates are denoted by a *hat* superscript.

3. WIDE-BAND ARRAY MODEL CONSISTENCY

A M sensor array of arbitrary geometry receives the signals radiated by D wide-band point sources. The array response to a wave-front impinging from direction characterized by the parameter vector $\boldsymbol{\theta}$ and angular frequency ω is the $M\times 1$ array *steering vector* [3] $\mathbf{b}(\boldsymbol{\theta},\omega)$. It is assumed for uniqueness that any set of $D<M$ steering vectors is linearly independent in an open neighborhood of the source directions $\{\boldsymbol{\theta}_1^T \ \cdots \ \boldsymbol{\theta}_D^T\}$.

Sensor outputs are down-converted by the frequency ω_0 and sampled at time $t=nT$, for $n=1,2,\dots N$, so that the steering vector $\mathbf{a}(\theta,\upsilon)$ at the discrete-time angular frequency $\upsilon=(\omega-\omega_0)T$ corresponds to

$$\mathbf{a}(\boldsymbol{\theta},\upsilon)=\mathbf{b}(\boldsymbol{\theta},\omega=\upsilon/T+\omega_0)\ . \tag{1}$$

The *array snapshot* $\mathbf{x}(n)$ stacks the complex envelopes of the sensor outputs $x_m(n)$, for $m=1,2,\dots,M$. If $E[\mathbf{x}(n)]=\mathbf{0}$ and the sum of the source signal correlation time and of the *overall length* $L\geq 1$ of the impulse responses between the signal and the sensors (measured from the first to the last non-zero sample across the array, *including coherent multipath*) is bounded by P, the *STCM* of order P, defined as [11]

$$\mathbf{R}_{ST}=E\left[\mathbf{x}_{ST}(n)\mathbf{x}_{ST}^H(n)\right]\ , \tag{2}$$

where $\mathbf{x}_{ST}(n)=\left[\mathbf{x}^T(n) \ \ \mathbf{x}^T(n+1) \ \ \cdots \ \ \mathbf{x}^T(n+P-1)\right]^T$ is the *space time snapshot* (STS), collects all the second order statistical information for real valued or circular complex signals and noise, assumed stationary within the observation time.

The STS model of a complex sinusoid $e^{j\upsilon n}$, impinging from direction $\boldsymbol{\theta}$ with steering vector $\mathbf{a}(\theta,\upsilon)$ is [10]

$$\mathbf{x}_{ST}(n)=\mathbf{E}(\upsilon)\mathbf{a}(\boldsymbol{\theta},\upsilon)e^{j\upsilon n}\ , \tag{3}$$

where $\mathbf{E}(\upsilon)=\left[\mathbf{I}_M \ \ \mathbf{I}_M e^{j\upsilon} \ \ \cdots \ \ \mathbf{I}_M e^{j(P-1)\upsilon}\right]^T$.

In particular, for $\upsilon_k=2\pi k/P$ and $k=0,1,\dots P-1$, $\mathbf{E}(\upsilon_k)^H\mathbf{E}(\upsilon_l)=P\mathbf{I}_M\delta_{kl}$ and the product $\mathbf{E}(\upsilon_k)\mathbf{y}$ for a generic vector $\mathbf{y}$ can be computed for all P values by a block *P*-point DFT. The model (3) is still *rank-one* with a *wide-band steering vector*

$$\mathbf{a}_{ST}(\boldsymbol{\theta},\upsilon)=\mathbf{E}(\upsilon)\mathbf{a}(\boldsymbol{\theta},\upsilon) \tag{4}$$

and is the basis for the following developments.

To demonstrate the *basic inconsistency* of periodogram based SCM estimation, the case of a single, generic, source signal $s(n)$ impinging from DOA $\boldsymbol{\theta}$ is considered, in absence of noise. Let $\mathbf{h}_m(\boldsymbol{\theta})=\left[h_m(0,\boldsymbol{\theta}) \ \cdots \ h_m(L-1,\boldsymbol{\theta})\right]^T$ be the impulse response between the *m*-th sensor output $x_m(n)$ and $s(n)$. Then, the *m*-th sensor output obeys

$$x_m(n)=\sum_{l=0}^{L-1}h_m(l,\boldsymbol{\theta})s(n-l)\ . \tag{5}$$

By well-known DFT convolution properties [9], the following decomposition holds:

$$\begin{aligned}\mathbf{x}_m(n)&=\left[x_m(n) \ \ x_m(n+1) \ \ \cdots \ \ x_m(n+P-1)\right]^T\\&=\mathbf{Q}\mathbf{A}_m(\boldsymbol{\theta})\boldsymbol{\Upsilon}\mathbf{s}_F(n)\end{aligned} \tag{6}$$

where $\mathbf{A}_m(\boldsymbol{\theta})=\text{diag}\left\{\left[A_{m,0}(\boldsymbol{\theta}) \ \cdots \ A_{m,N_F-1}(\boldsymbol{\theta})\right]\right\}$ stores on its main diagonal the $N_F\geq P+L-1$ DFT samples $A_m(k,\boldsymbol{\theta})$ of the zero padded $\mathbf{h}_m(\boldsymbol{\theta})$, $\mathbf{s}_F(n)$ is the N_F point DFT of $\left[s(n-L+1) \ \cdots \ s(n+N_F-L)\right]^T$, $\boldsymbol{\Upsilon}=N_F^{-1}\text{diag}\left(\left[1 \ \ e^{j2\pi L/N_F} \ \ \cdots \ \ e^{j2\pi L(N_F-1)/N_F}\right]\right)$ and $\mathbf{Q}$ is a matrix of size $P\times N_F$ with orthogonal rows and entries $\mathbf{Q}(p,k)=e^{j2\pi pk/N_F}$. The STCM $\mathbf{R}_{ss}$ of the source (6) is, up to a permutation matrix $\mathbf{T}$,

$$\mathbf{R}_{ss}=\mathbf{T}\begin{bmatrix}\mathbf{Q}\mathbf{A}_1(\boldsymbol{\theta})\\ \vdots\\ \mathbf{Q}\mathbf{A}_M(\boldsymbol{\theta})\end{bmatrix}\left[\boldsymbol{\Upsilon}\mathbf{P}_{ss}\boldsymbol{\Upsilon}^H\right]\begin{bmatrix}\mathbf{Q}\mathbf{A}_1(\boldsymbol{\theta})\\ \vdots\\ \mathbf{Q}\mathbf{A}_M(\boldsymbol{\theta})\end{bmatrix}^H\mathbf{T}^T \tag{7}$$

where $\mathbf{P}_{ss}=E\left[\mathbf{s}_F(n)\mathbf{s}_F(n)^H\right]$ is the *two-sided DFT* of the auto-correlation matrix of length N_F-1 of $s(n)$.

Since $\mathbf{R}_{ss}$ can have a rank up to $L+P-1$ from (5) and (6) [11], in general it *cannot be exactly fitted* by the P steering vectors $\mathbf{a}_{ST}(\boldsymbol{\theta},\upsilon_k)$ for $k=0,1,\dots,P-1$, as assumed by classical binning estimators [2], [6], for any sample size and SNR.

The classical SCM at frequency υ_k is $\mathbf{R}_{ss}(\upsilon_k)=P^{-1}\mathbf{E}(\upsilon_k)^H\mathbf{R}_{ss}\mathbf{E}(\upsilon_k)$ after DFT filtering [2]. It does not cancel any component of $\mathbf{s}_F(n)$ after the products $\begin{bmatrix} 1 & e^{-j\upsilon_k} & \cdots & e^{-j(P-1)\upsilon_k} \end{bmatrix} \mathbf{Q}\mathbf{A}_m(\boldsymbol{\theta})$, so that the source signature within the k th bin cannot have rank one.

At low SNR, these mismatch errors may fall harmlessly below the SCM noise floor, but at high SNR they show up as un-calibrated ghost sources [8], setting a lower bound to the DOA variance for random sources.

4. ST-MUSIC SIGNAL SUBSPACE

The ST-MUSIC approach starts from the eigen-decomposition (EVD) of $\mathbf{R}_{ST}$ [10], [11] in the presence of white background noise with STCM $\mathbf{R}_{vv} = \lambda_v \mathbf{I}_{MP}$:

$$\mathbf{R}_{ST} \overset{EVD}{=} \mathbf{E}_s \boldsymbol{\Lambda}_s \mathbf{E}_s^H + \lambda_v \mathbf{E}_v \mathbf{E}_v^H \tag{8}$$

where $\boldsymbol{\Lambda}_s = \operatorname{diag}\left(\begin{bmatrix} \lambda_1 & \cdots & \lambda_\eta \end{bmatrix}\right)$, $\lambda_1 \geq \lambda_2 \geq \ldots \geq \lambda_\eta > \lambda_v$, $\mathbf{E}_s$ is an orthogonal basis for the *wide-band signal subspace* (WSS) of rank η, and its orthogonal complement $\mathbf{E}_v$ spans the *wide-band noise subspace* (WNS) [10]. Several techniques are available for estimating η from sample data [7], [10].

For the single source case (7), $\mathbf{E}_s$ has the structure

$$\mathbf{E}_s = \mathbf{T} \begin{bmatrix} \mathbf{Q}\mathbf{A}_1(\boldsymbol{\theta}) \\ \vdots \\ \mathbf{Q}\mathbf{A}_M(\boldsymbol{\theta}) \end{bmatrix} \mathbf{C}_s \tag{9}$$

where the $N_F \times \eta$ matrix $\mathbf{C}_s$ has the same numerical rank of $\mathbf{R}_{ss}$, i.e., $\eta \leq L + P - 1$.

The ST-MUSIC for white noise [10] solves at each ν_k the *Generalized Least Squares* problem [13]

$$\mathbf{E}_s \mathbf{W}_k = P^{-1/2} \mathbf{E}(\upsilon_k) \mathbf{Y}_k + \mathbf{B}_k \mathbf{Z}_k \tag{10}$$

where $\mathbf{W}_k$ is the unknown weight matrix of size $\eta \times \eta_k$ for fitting the *wideband steering vector basis* $P^{-1/2}\mathbf{E}(\upsilon_k)\mathbf{Y}_k$ of rank $\eta_k < M$ in a MUSIC fashion, $\mathbf{B}_k$ is the *orthogonal complement* of $\mathbf{E}(\upsilon_k)$ and spans the union of all the $P-1$ subspaces $\mathbf{E}(\upsilon_i)$ for $i \neq k$, and $\mathbf{Z}_k$ is the *spectral leakage term* to be minimized in the Least Squares sense.

By inserting (9) into *(10)* it is evident that if $\mathbf{W}_k$ lies in the null space of $\mathbf{B}_k^H \mathbf{E}_s$, $\mathbf{Z}_k = \mathbf{0}$ and $\mathbf{Y}_k$ can only be made by *linear combinations* of steering vectors $\mathbf{a}(\boldsymbol{\theta}_d, \upsilon_k)$, restoring the narrow-band model and therefore the *consistency* of the signal subspace estimate given *sufficient* M and P. For instance in (9) *perfect leakage nulling* and a *rank one* $\mathbf{Y}_k$ can be achieved when $\mathbf{C}_S$ is full rank (as in the case of random stationary signals), $P > L$ and $(P-1)M \geq L + P - 1$, but ST-MUSIC consistency holds in most multi-source scenarios.

Under the constraint $\mathbf{Y}_k \mathbf{Y}_k^H + \mathbf{Z}_k \mathbf{Z}_k^H = \mathbf{I}_M$, the solution of (10) is given by the following *reduced size* SVD [13]

$$\mathbf{F}_k = P^{-1/2} \mathbf{E}(\upsilon_k)^H \mathbf{E}_s \overset{SVD}{=} \mathbf{U}_k \boldsymbol{\Sigma}_k \mathbf{W}_k^H \Rightarrow \mathbf{Y}_k = \mathbf{U}_k \boldsymbol{\Sigma}_k \; . \tag{11}$$

In the case of perfect leakage nulling, $\mathbf{F}_k$ would have $\eta_k \leq D$ *unit* singular values in the diagonal matrix $\boldsymbol{\Sigma}_k$ of size $M \times \eta$ [10]. The other singular values are *zero*. Partial nulling arises because of noise effects, STCM estimation errors and sources radiating pure tones or cyclo-stationary signals, but *empirical singular values* very close to one indicate high concentration of signal energy in the analyzed bin and therefore low expected DOA errors. In the sequel, the properties of the finite sample ST-MUSIC subspace estimate are investigated to derive the statistically optimal subspace weighting.

5. OPTIMAL ST-MUSIC SUBSPACE WEIGHTING

The STCM estimate is built by either $K \approx N/P \gg M$ independent STSs, or by sample cross-correlations among sensor output sequences of length N [11]. The latter estimate has faster statistical convergence, better behavior with non-stationary signals and less bias, but empirically exhibited *quite similar large sample accuracy* as the former one, at least for stationary signals [10], [11].

For Gaussian signals and noise, the asymptotic $O\left(K^{-1/2}\right)$ perturbation of the sample WSS $\hat{\mathbf{E}}_s$, estimated from K independent snapshots, can be written as $\hat{\mathbf{E}}_s = \mathbf{E}_s\left(\mathbf{I}_\eta + \mathbf{G}_s\right) + \mathbf{E}_v \mathbf{G}_v$ [7], where the random, zero mean *cosine matrices* $\mathbf{G}_s = -\mathbf{G}_s^H$ and $\mathbf{G}_v$ respectively describe an inessential *random rotation of the WSS* and the *sample WSS leakage into the WNS*, which generates the DOA estimation errors [5], [7], [8]. The entries $\mathbf{G}_v(k,l)$ for $K \to \infty$ approach zero mean, circular Gaussian variables with covariances [5]

$$\begin{gathered} E\left[\mathbf{G}_v(k,l)\mathbf{G}_v^*(m,n)\right] \simeq \\ \frac{\delta_{km}\delta_{ln}\lambda_v\lambda_l}{K(\lambda_l - \lambda_v)^2} = \delta_{km}\delta_{ln}\frac{\rho_l}{K} \end{gathered} \tag{12}$$

for $k, m > \eta$ and $0 \leq l, n \leq \eta$, and $E\left[\mathbf{G}_s(k,l)\mathbf{G}_v^*(m,n)\right] = 0$.

The *empirical* $\mathbf{F}_k$, indicated by $\hat{\mathbf{F}}_k$, is decomposed by the *Generalized SVD* theorem [13] as

$$\begin{gathered} \hat{\mathbf{F}}_k \overset{def}{=} P^{-1/2} \mathbf{E}^H(\nu_k) \hat{\mathbf{E}}_S \overset{SVD}{=} \hat{\mathbf{U}}_k \hat{\boldsymbol{\Sigma}}_k \hat{\mathbf{W}}_k^H \simeq \\ \mathbf{U}_k \boldsymbol{\Sigma}_k \mathbf{W}_k^H \left(\mathbf{I}_\eta + \mathbf{G}_s\right) + \mathbf{U}_k \boldsymbol{\Gamma}_k \mathbf{V}_k^H \mathbf{G}_n \end{gathered} \tag{13}$$

where $P^{-1/2}\mathbf{E}(\nu_k)^H \mathbf{E}_v \overset{SVD}{=} \mathbf{U}_k \boldsymbol{\Gamma}_k \mathbf{V}_k^H$ and $\boldsymbol{\Gamma}_k \boldsymbol{\Gamma}_k^T = \mathbf{I}_M - \boldsymbol{\Sigma}_k \boldsymbol{\Sigma}_k^T$. If the spectral leakage of *all* sources can be nulled, $\boldsymbol{\Sigma}_k$ has rank $\eta_k \le D$. So the first term in (13) by (11) represents an inessential random rotation of $\mathbf{Y}_k$, while by the term $\mathbf{U}_k \boldsymbol{\Gamma}_k \mathbf{V}_k^H \mathbf{G}_n$ asymptotically generates a *spatially white noise* in $\mathbf{U}_{vk}$, the orthogonal complement of $\mathbf{Y}_k$.

The *ST-MUSIC* subspace, weighted by a generic Hermitian, positive semi-definite matrix $\mathbf{P}_k$ as

$$\hat{\mathbf{R}}_{ss}(\upsilon_k) = \hat{\mathbf{F}}_k \hat{\mathbf{W}}_k \mathbf{P}_k \hat{\mathbf{W}}_k^H \hat{\mathbf{F}}_k^H = \hat{\mathbf{Y}}_k \mathbf{P}_k \hat{\mathbf{Y}}_k^H \quad , \qquad (14)$$

is characterized for $K \to \infty$ by

$$E\left[\hat{\mathbf{R}}_{ss}(\nu_k)\right] \simeq \mathbf{Y}_k \mathbf{P}_k \mathbf{Y}_k^H + K^{-1}\lambda_v \operatorname{trace}\left(\mathbf{W}_k^H \boldsymbol{\Psi} \mathbf{W}_k \mathbf{P}_k\right) \mathbf{U}_{vk} \mathbf{U}_{vk}^H$$

where $\boldsymbol{\Psi} = \operatorname{diag}\left(\begin{bmatrix}\rho_1 & \cdots & \rho_\eta\end{bmatrix}\right)$. The optimal $\hat{\mathbf{P}}_k$ in the WSF sense minimizes the asymptotical error variance of (14) in a Gaussian ML fashion [5], by setting

$$\hat{\mathbf{P}}_k \propto \arg\min_{\mathbf{P}} \left[\ln\det(\mathbf{P}) + \operatorname{trace}\left(\hat{\mathbf{W}}_k^H \hat{\boldsymbol{\Psi}} \hat{\mathbf{W}}_k \mathbf{P}\right)\right] \qquad (15)$$

leading to $\hat{\mathbf{P}}_k \propto \left(\hat{\mathbf{W}}_k^H \hat{\boldsymbol{\Psi}} \hat{\mathbf{W}}_k\right)^{-1}$. The optimal ST-MUSIC II weighted subspace $\hat{\mathbf{R}}_{ss}(\upsilon_k)$ is obtained by truncating at rank $\eta_k < M$ the EVD of the *pseudo-SCM*

$$\hat{\mathbf{R}}_{xx}^{(MUSIC)}(\upsilon_k) = \hat{\mathbf{Y}}_k \left(\hat{\mathbf{W}}_k^H \hat{\boldsymbol{\Psi}} \hat{\mathbf{W}}_k\right)^{-1} \hat{\mathbf{Y}}_k^H \quad . \qquad (16)$$

The earlier ST-MUSIC [10] used a similar weighting, but derived from (13) after retaining only the η_k largest singular values of $\hat{\mathbf{F}}_k$ very close to unity.

Finally, a set of $\hat{\mathbf{R}}_{ss}(\upsilon_k)$ computed by (11), (15) and (16) can replace the SCMs in *any* wide-band WSF [2] or CF estimators, such as the near optimal WAVES [7] used in the following simulations.

6. COMPUTER SIMULATIONS

The proposed ST-MUSIC II was compared with the classical SCM approach [6], [7] and the earlier ST-MUSIC [10] in the same basic scenario of [6], [7]. Four Gaussian sources impinged on a linear array with $M = 8$ sensors, half-wavelength spaced at 100 Hz, from angles 8°, 13°, 33° and 37°, referred to broadside, and were generated by an accurate *time domain* simulator. Spatially and temporally white Gaussian noise was added to give SNR in the range $[-5, 40]$ dB, referred to each sensor. $N = 6400$ samples were collected in the band $(60,140)$ Hz at rate $T^{-1} = 80$ Hz for each of the 500 Monte Carlo runs for each SNR, to get $P = 64$ bins and $K = 100$ independent snapshots. The 33 bins in the band $(80,120)$ Hz were used for DOA estimation by WAVES [7] coupled with MODE [14] and unitary focusing matrices [6], selecting $\eta_k = 4$.

The DOA sample variance for the (most difficult) source at 37° was depicted in Figs. 1-3. Fig. 1 shows the results for four equi-powered, uncorrelated, white sources, together with the Cramer-Rao Bound (CRB) and the *perfect focusing* WAVES bound [7]. In Fig. 2, the sources from 13° and 33° were replaced by AR [9] processes generated by filtering white noise through filters with transfer functions $\left(1\text{-}0.9\mathrm{e}^{j\pi/3}z^{-1}\right)^{-1}$ and $\left(1\text{-}0.9\mathrm{e}^{-j\pi/4}z^{-1}\right)^{-1}$. SNR was referred to the excitation noise variance.

Finally, Fig. 3 shows the results for a strongly coherent multipath scenario, where the wave-fronts impinging from 13° and 37° carried replicas delayed by $0.45T$ and $0.35T$ of the equi-powered, white signals radiated by the sources at 8° and 33°. As expected, the numerical rank of each ST-MUSIC subspace was $\eta_k = 2$ (i.e., the number of uncorrelated signals). The best overall results were obtained by using *robust weights* for WAVES [7] and only two signal eigenvectors in the final MODE DOA estimator, which resolved coherent multipath [14].

The *recovery of consistency* obtained by ST-MUSIC algorithms was clearly demonstrated by the absence of the DOA variance plateau at high SNR, and by the *ultimate accuracy* increased up to 20 dB with respect to SCM based counterparts. At low SNR, the ST-MUSIC II performance was similar to the SCM one, already close to the CRB [6]. The earlier ST-MUSIC [10] was mostly penalized by the preliminary selection of the subspace ranks η_k. However, as shown in Fig. 3, with strongly coherent sources the original ST-MUSIC criterion may prevent inclusion of components affected by significant leakage and bias.

7. CONCLUSION

Basic model inconsistency undermines the theoretical foundation of earlier wide-band DOA estimators based on frequency binning, especially in difficult multi-source scenarios characterized by wide SNR ranges and non-white source signals. The ST-MUSIC methods avoid this pitfall at high SNR, while the novel ST-MUSIC II weighting scheme recovers the near-optimal low SNR performance, typical of classical CF estimators.

REFERENCES

[1] M. R. Azimi-Sadjadi, Y. Jiang, G. Wichern, "Properties of randomly distributed sparse acoustic sensors for ground vehicle tracking and localization," *Proc. of SPIE'06 Defense and Security Symposium*, vol. 6201, Orlando, FL,

USA, April 17, 2006.

[2] M. G. M. Hussain, “Principles of space-time array processing for ultrawide-band impulse radar and radio communications,” *IEEE Trans. on Vehicular Technology*, vol. 51. no. 3, pp. 393-403, May 2002.

[3] P. M. Schultheiss and H. Messer, “Optimal and suboptimal broad-band source location estimation,” *IEEE Trans. on Signal Processing*, vol. 41, no. 9, pp. 2752–2763, Sept. 1993.

[4] J. A. Cadzow, “Multiple source location - The signal subspace approach,” *IEEE Trans. Acoust., Speech, Signal Processing*, vol. 38, no. 7, pp. 1110–1125, July 1990.

[5] M. Viberg, M. Ottersten, and T. Kailath, “Detection and estimation in sensor arrays using weighted subspace fitting,” *IEEE Trans. on Signal Processing*, vol. 39, no. 11, pp. 2436-2499, Nov. 1991.

[6] H. Wang and M. Kaveh, “Coherent signal subspace processing for the detection and estimation of angles of arrival of multiple wideband sources”, *IEEE Trans. on Acoustics, Speech and Signal Proc.*, vol. 33, no. 8, pp. 823-831, Aug. 1985.

[7] E. D. Di Claudio, R. Parisi, “WAVES: weighted average of signal subspaces for robust wideband direction finding,” *IEEE Trans. on Signal Processing*, vol. 49, no. 10, pp. 2179-2191, Oct. 2001.

[8] E. D. Di Claudio, "Asymptotically perfect wideband focusing of multi-ring circular arrays", *IEEE Trans. on Signal Processing*, Vol. 53, no. 10, Part I, pp. 3661-3673, Oct. 2005.

[9] S. M. Kay, *Modern Spectral Estimation*: *Theory and Application*, Prentice Hall, 1988.

[10] E. D. Di Claudio, G. Jacovitti, “Wideband source localization by Space-Time MUSIC subspace estimation,” *Proc. of the 8th Int. Symp. on Image and Signal Processing and Analysis (ISPA 2013)*, pp. 324-329, Trieste, Italy, 4-6 Sept. 2013.

[11] G.H. Niezgoda, J. Krolik, “The application of adaptive multichannel spectral estimation for broadband array processing,” *Proc. of the 1991 Int. Conf. on Acoustics, Speech, and Signal Processing, 199 (ICASSP-91)*, vol. 2, pp. 1397-1400, 14-17 Apr. 1991.

[12] E. D. Di Claudio, R. Parisi, “Robust ML wide-band beamforming in reverberant fields,” *IEEE Trans. on Signal Processing*, vol. 51, no. 2, pp. 338–349, Feb. 2003.

[13] G. Golub, C. F. Van Loan, *Matrix Computation*, John Hopkins, II ed., 1989.

[14] P. Stoica, K. C. Sharman, “Novel eigenanalysis method for direction estimation,” *Radar and Signal Processing, IEE Proceedings Part F* , vol. 137, no. 1, pp. 19-26, Feb. 1990.

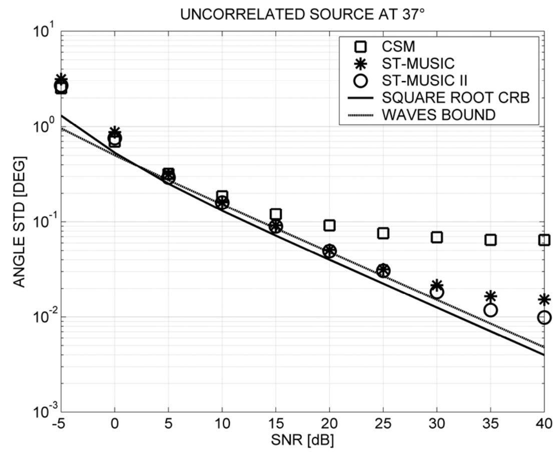

Fig. 1 Sample DOA standard deviation, square root CRB and perfect subspace mapping bound [7] for the source at 37° in the uncorrelated source case.

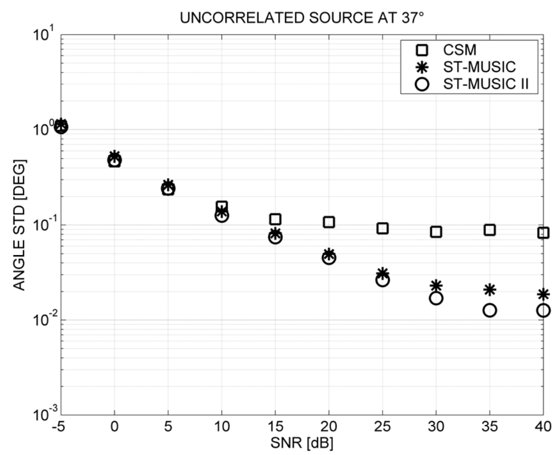

Fig. 2 Sample and DOA standard deviation of the source at 37° in the colored source case.

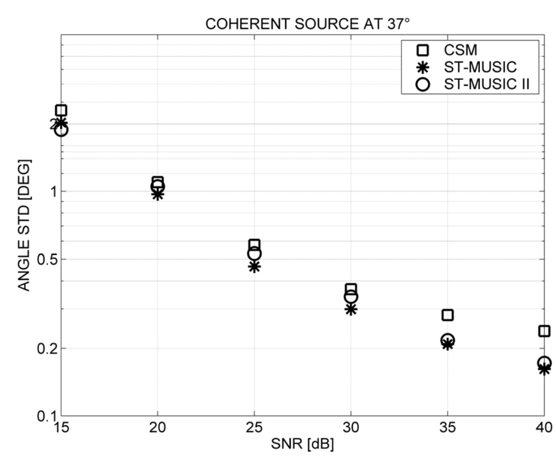

Fig. 3 Sample DOA standard deviation of the source at 37° in the coherent source case.